Penerbit Akademia Baru

Journal of Advanced Research in Fluid Mechanics and Thermal Sciences

Journal homepage: www.akademiabaru.com/arfmts.html
ISSN: 2289-7879

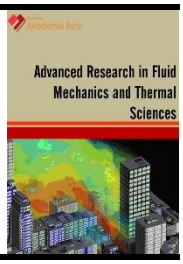


# Effect of Porous Media on The Performance Characteristics of a Concentric Vertical Annular Tube

Open Access

Mustafa Fouad Yousif[1,*], Saad Najeeb Shehab[1], Hayder Mohammad Jaffal[1]

[1] Mechanical Engineering Department, College of Engineering, Mustansiriyah University, Baghdad, Iraq

**ARTICLE INFO**

***Article history:***
Received 31 December 2019
Received in revised form 5 February 2020
Accepted 6 February 2020
Available online 15 September 2020

**ABSTRACT**

In this work, energy analyses were performed to enhance the characteristics and performance of forced convection into vertical annuli with and without porous media. Different sizes of porous media and porosities were used. A three-dimensional numerical simulation of an annular tube with and without porous medium was conducted using ANSYS Fluent software version 17.2. Water liquid was used for Reynolds numbers ranging from 100 to 600 and a wide range of wall heat flux. In the experiment, an annular tube consisting of two concentric cylinders 300 mm long was manufactured. The outer cylinder was made of Teflon, whereas the inner cylinder was made of copper. The inner cylinder had an outer diameter of 20 mm, and the outer cylinder had an inner diameter of 100 mm. Three different porous medium diameters (11, 16 and 25 mm) and three different porosities (0.65, 0.75 and 0.85) were used and tested under steady state to study fluid flow and the heat-transfer properties of the annular tube. Results of the energy analysis indicated that Nusselt number values increased with decreased porosity (i.e., by approximately 4.25, 4.2 and 3.5 times at the porosities of 0.65, 0.75 and 0.85, respectively) compared with those in the annulus without glass balls as porous media at the same glass sphere sizes. Accordingly, the best Nusselt number improvement occurred at the diameter of 16 mm (approximately 4.6 times) and at the lowest porosity of 0.65 (approximately 4.25 times).

***Keywords:***
Porous medium; Annular tube; Heat transfer improvement; Performance factor; CFD



## 1. Introduction

Enhancement in heat transfer using porous media is attracting research attention because of their ability to dissipate a substantial amount of heat. In particular, emphasis has been given on improving heat transfer using porous media in many engineering applications. Recently, the hydrothermal characteristics through an annulus filled with porous media have been investigated in many engineering applications such as in heat exchangers, electronic devices, nuclear reactors, solar absorbers, geothermal and storage thermal systems, etc. Bu-Xuan and Jian-Hua [1] experimentally

* *Corresponding author.*
*E-mail address: mustafamf94@yahoo.com*

https://doi.org/10.37934/arfmts.75.2.94112

investigated the influence of porous particles size on thermal performance of a vertical annular. Their results (for oil or water) indicted that the Nusselt number is highly influenced using porous due to flow disturbance. Yang *et al.,* [2] investigated theoretically heat transfer characteristics of a horizontal annual filled with porous medium. The outer surface assumed to be adiabatic while the inner surface subjected to uniform heat flux. As an example, illustration in views, the air and Aluminium foam composition were chosen. Chikh and Allouache [3] studied the turbulent flow performance into an annular pipe. heat exchanger filled with porous inserts by entropy generation minimization technique. They used a modified k-ε model to calculate the turbulence into porous media. They concluded the heat transfer enhancement about 40% for the porous inserts. Cui *et al.,* [4] have performed a numerical study of porous annuli thermoelectric generators at waste thermal harvesting. They considered electrical and heat contact resistance between the heat sink and thermoelectric generator to compute the power output. They suggested correlation equation between porosity for peak output power and pore diameter of thermoelectric generators. Shirvan *et al.,* [5,6] have investigated numerically analysis heat transfer into double-pipe heat exchanger filled with porous media. They utilized k-ε and Darcy-Brinkman- Forchheimer models to evaluate the effectiveness of heat exchangers and heat transfer for wide range of Reynolds and Darcy numbers. They showed that the sensitivity of effectiveness for heat exchangers is positive with Reynolds number and negative with Darcy number. Nimvari *et al.,* [7] studied the turbulence influence on the heat performance of porous layer pipe. They simulated laminar and turbulent flows into a pipe partially filled with porous layer. They showed that the turbulence influence in porous zone is very important at layer thickness of porous layer. Rong *et al.,* [8] numerically simulated the enhancement of heat transfer into a pipe filled with porous medium. They used axisymmetric Lattic Boltzman model to compute the fluid flow and heat characteristics. They found that the porous media thickness enhances the thermal performance. Many researchers have numerically studied the heat transfer and flow performance and characteristics inside a pipes and annulus using porous media under free, forced, and mixed heat convection [9-14]. Generally, they found that the porous media improve the heat performance with undesirable increases in pressure losses. The present study aims are to evaluate the thermal and hydraulic performance characteristics of a concentric vertical annular tube filled with a porous medium. Develop 3D numerical simulation using ANSYS Fluent software to investigate the effects of different geometrical and physical parameters on the heat performance of the concentric vertical annular tube. The geometrical parameters include the diameter of porous media and porosity in addition the physical parameters like the Reynolds number and heat flux are studied. Utilize an experimental test rig of the concentric vertical annular tube using glass balls as porous media and water as working fluid to validate the numerical simulation.

## 2. Numerical Work

### *2.1 Physical Model of Annular Tube*

The concentric annular tube filled with a porous medium has two computational domains. The first one is the solid domain, which includes the inner copper tube and porous material (glass balls); the second domain represents the liquid (water) in the annular tube. The annular tube consists of two external and internal cylinders having multiple axes with fluid flow, as shown in Figure 1. The geometry of the two cylinders includes the length of the two cylinders (L), the diameter of the external cylinder (Do), the diameter of the internal cylinder heated by the thermal source (Di), the diameter of the glass balls (d) representing the porous material and the thickness of the cylinders (t). The diameter wall of the inner cylinder is heated under thermal flux. The liquid used (water) is at variable speed with constant temperature input (300 K). A thermal transfer of heat occurs between

the surface of the internal cylinder heated with water and porous material in levels x, y and z. Through the materials used, the water is selected as a factor from the fluent material database, and copper is selected as heat-heated with heat conductivity of 387.6 W/ (m.K).

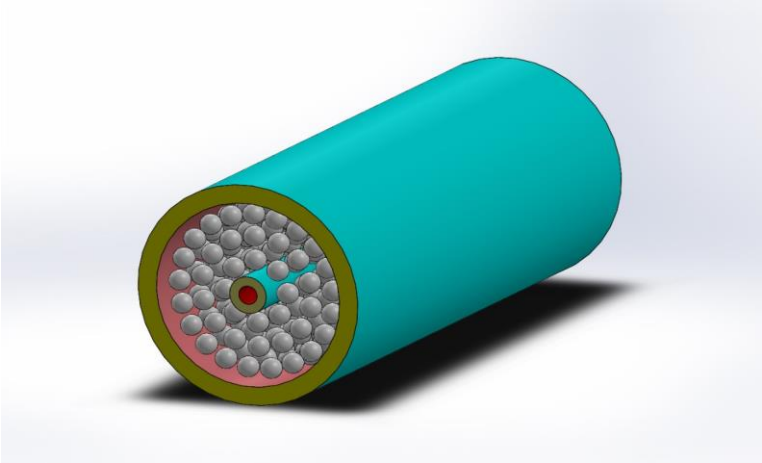

**Fig. 1.** Schematic diagram a vertical concentric annular tube containing glass balls

*2.2 Computational Model of Annular Tube*

ANSYS Fluent software version 17.2 used to perform the simulation. Darcy's flow model (Brinkman) used in this work. The Solid Works version (18) software is used to create a 3D geometric model of the concentric vertical annular tube filled with a porous medium (glass balls) to provide thermal hydraulic analysis in this work. Figure 1 depicts two zones of heat transfer. The first zone is restricted in the copper cylinder where the conduction heat transfer is predominant. The second zone is the porous medium where two of heat transfer mechanisms are predominant; conduction within porous media and convection within fluid flow region.

*2.3 Governing Equations and Boundary Conditions*

For the steady, single-phase, incompressible, laminar flow, and laminar forced convection heat transfer in the annular tube, the following governing equations must be solved [15].

Continuity equation

$$\rho_f \nabla . \vec{U} = 0 \tag{1}$$

Momentum equation

$$\frac{\rho_f}{\varepsilon^2}\left(\nabla . \vec{U}\right)\vec{U} = -\nabla P + \rho_w g - \gamma\left[\frac{\mu_f}{K} + \frac{\rho_f C_{p,f}}{\sqrt{K}}\left|\vec{U}\right|\right] + \frac{\mu_f}{\varepsilon}\nabla^2\vec{U} \tag{2}$$

where $\mu_w$ and $\rho_w$ are the dynamic viscosity and density of water, respectively; and P is the local fluid pressure.

Energy equation

$$\rho_f Cp_f\left(\vec{U}.\nabla T\right) = k\nabla^2 T \quad (3)$$

where $C_p$f and k are the specific heat and thermal conductivity of water, respectively; and T is the local fluid temperature.

A range of boundary conditions must be used to complete the solution. For good solutions, boundary conditions must be specified and used as a rule in the light of physics. The boundary conditions are chosen to be synonymous with the actual flow conditions used in the tests. For fluid flow and heat transfer, the types of boundary conditions are inlet, outlet and thermal boundary conditions. Table 1 represents the limits of these terms used.

**Table 1**
Boundary conditions of fluid flow and heat transfer for CFD simulation

| | Hydraulic simulation | Thermal simulation |
|---|---|---|
| Inlet | Velocity inlet | Constant temperature at 300 K |
| Outlet | Zero-pressure outlet | $\frac{\partial T}{\partial z} = 0$ |
| Outer surface | No slip wall | Adiabatic wall |
| Porous surface | No slip wall | Adiabatic wall |
| Inner surface | No slip wall | $k_s \frac{\partial Ts}{\partial n} = q''$ |

*2.4 Numerical Simulation*

One of the most important stages in the simulation is the grid creation. The grid is geometrically small and covers the entire physical area. The purpose of this grid is to determine the separate sizes, so that conservation laws can be implemented. The first stage is the calculation of the numerical solutions of equations that describe the physical process of grid generation. The result of the solution is determined by the grid quality. Improving the solution quality can lead to the creation of another grid, whereas the use of an undeveloped grid leads to deviations in the solution. Mesh cells are matched to the boundary surface, and other areas of flow are identified using flexible elements. Figure 2 illustrates the arithmetic grid distribution of the model.

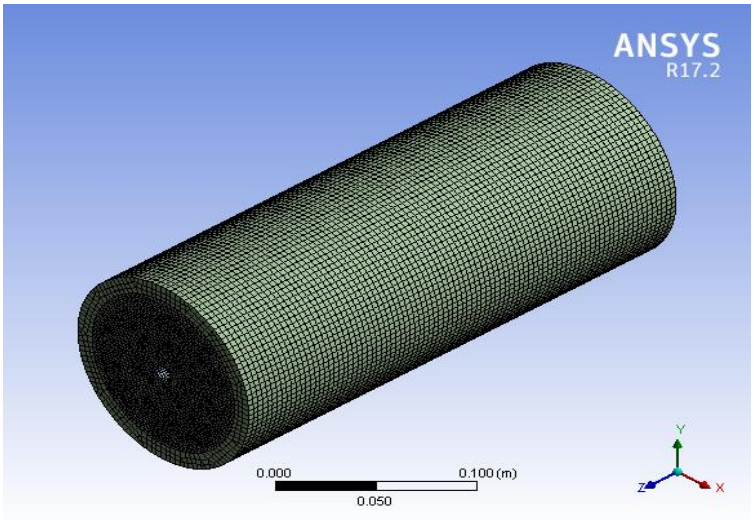


**Fig. 2.** Grid generation for the annular tube geometry

A test of grid independence is performed to obtain the best grid structures that provide accurate results. The annular tube grids are established in the application of the ANSYS grid. Simulation accuracy is improved by using a computer with an accurate grid file, which can be obtained by studying grid independence. A grid study is conducted via the following steps. Firstly, a preliminary analysis of the grid and the recording of the temperature over time of the annular tube are conducted. Secondly, re-arrangement with a more accurate grid and the same boundary conditions is performed. Thirdly, grid independence is evaluated by monitoring one point over time using all grid sizes. The process is performed more than once to obtain an accurate and acceptable affinity. Grids sensitivity are tested at the Re = 600 for three diameters (11, 16 and 25 mm), and the results are presented in Figure 3.

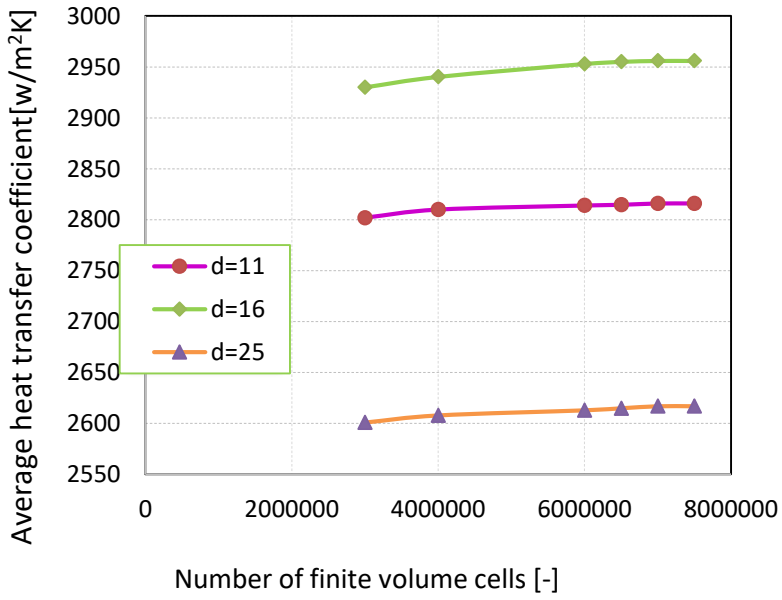


**Fig. 3.** Average heat-transfer coefficient variation as a function of the number of finite volume cells

Using a finite volume technique, the governing equations with their boundary conditions are numerically resolved. On the basis of finite volume method, the iterative solution for arithmetical conditions is performed using ANSYS-Fluent (version 17.2) software. To calculate the flow domain, a laminar model is constructed. The SIMPLE algorithm is used for coupling velocity and pressure components. By a second-order upwind scheme, momentum and energy equations are discretized. The solution becomes convergent when the residuals are less than 10−6.

## 3. Experimental Work

### *3.1 Experimental Test Rig*

Figure 4 illustrates the especially manufactured experimental test rig for this work. The main components of the test rig are test loop, test section consisting of a concentric vertical annular tube filled with a porous medium and measurement tools.

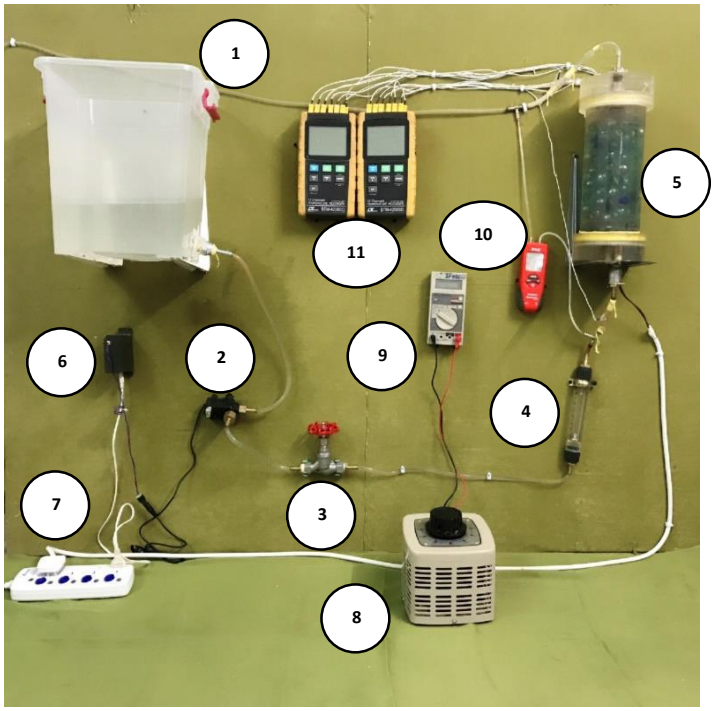


**Fig. 4.** Photograph of experimental test rig: (1) Water tank (2) Pump (3) Valve (4) Flow meters (5) Test section (6) AC Power supply (7) DC power supply (8) Voltage regulator (9) Digital multi-meter (10) Manometer (11) Temperature recorders

### *3.1.1 Test loop*

The test loop consists of a water tank with water piped out to flow to the centrifuge pump. When running the pump, the water goes through the tubes to the valve which controls the amount of water going out to the water flow meter. The flow meter is used to control the flow of water, and several rates are used for different volumetric flows ranging from 0.3 l/m to 1.9 l/m. This condition is consistent with Re values ranging from 100 to 600. The water then comes out by pipes into two branches, namely, a pipe that enters the test section and a pipe to a pressure gauge to measure the inlet pressure. The water entering the test section is heated by the heater, and then the hot water comes out to two branches. Hot water comes out of the system and a pipe into the pressure gauge to measure the outlet pressure.

### *3.1.2 Test section*

The test section is made of a concentric annular tube filled with a porous medium, the glass balls. The annular tube consists of two cylindrical concentric tubes with an outer cylinder and an internal cylinder. The glass balls are located at the space between the two cylinders, as shown in Figure 5(a) and 5(b). The outer cylinder is made of Teflon material with a length of 300 mm. The diameter of the external cylinder is 120 mm, and the inner diameter of the outer cylinder is 100 mm. Teflon material is chosen, because it is a good insulation unaffected by heat; it also presents resistance to corrosion and no adhesion. A solid Teflon cylinder is taken. The cylinder is drilled in accordance with its length by a drilling machine, as shown in Figure 5(a) and 5(b). The surface of the outer drum is drilled by a hole machine with a diameter of 3 mm to place the thermocouples on the surface of the outer cylinder. Six holes are excavated; the first one is for a 40 mm-long cylinder, and the rest are at a

distance of 44 mm. Threaded Teflon caps are used to cover both sides of the test section. Two covers of Teflon (150 and 50 mm thickness) are manufactured to seal the cylinder from both sides to prevent water leakage during the flow when the pump is turned on and the exit of the glass balls and to be a support for the inner cylinder, where a screw tooth is made for both sides. They cover are also drilled by a perforation machine to allow water to enter and exit, for the exit of thermocouple wire and to place the internal cylinder. The inner cylinder is made of copper material with a length of 400 mm, where the length of 300 mm represents the test section, and the remaining length of 100 is for the Teflon cover, the outer diameter of the inner cylinder (20 mm) and the internal diameter (10 mm). The thermocouples are installed on the outer surface of the inner cylinder. The distance on which the thermocouples are installed is the same distance as that for the thermocouples of the external cylinder. They are coated with a thermal adhesive to prevent the water effect during the flow when the pump is running.

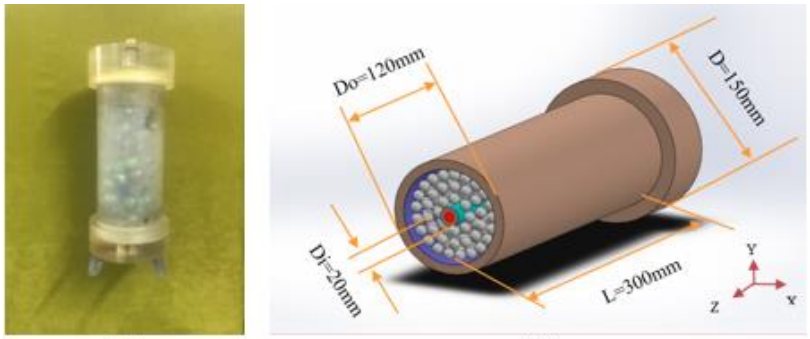


**Fig. 5.** Photograph and 3D schematic of the test section

Several different tests are performed to study the effect of porous media on the performance of the annular tube. Different parameters are used to measure their effect on heat transfer, three diameters (11, 16 and 25 mm) are used for glass balls, and three porosity values (0.65, 0.75 and 0.85) are adopted. Water flow rates are used depending on Re ranging from 100 to 600, and different heat fluxes (1.7–20.2 kW/m$^2$) are used. The main steps of the experimental procedure are as follows: (1) The heater is inserted into the inner cylinder of the test section and other parts of the test rig. (2) The water tank is fully filled with water. (3) After running the pump, the water flow is adjusted to the required value by using a valve to control the water quantity. (4) A power supply unit is turned on to supply the electric heater, when the required heat flow is needed to the inner surface of the internal cylinder by adjusting the input voltage using the power supply DC. (5) Every 10 min, the temperature is recorded when the steady state is reached, i.e., when the temperature is observed at fixed value. The time required to reach the steady state is approximately 30 min. (6) After reaching the stable state, the water temperature at the input and outlet of the annular tube is measured. Water flow rate, current, voltage and pressure drop in water are then measured. (7) Steps 3–6 are repeated for each condition to cover all water flow rates and heat flux. (8) Steps 1–7 are repeated to use different porosity values and diameters for glass balls.

### *3.2 Data Processing*

The total heat absorbed by the fluid by the electrical input ($q_{in}$) of the heating element inside the annular tube can be represented by the heat produced by the heater as a result of current and voltage, i.e.,

$$q_{in} = q_{ele} = I \times V \tag{4}$$

where I is the input current, and V is the input voltage. The net heat gain is determined by the heat loss from the supplied electrical power, i.e.,

$$q = q_{ele} - q_{loss} = \mathring{m}Cp_f(T_{f,out} - T_{f,in}) \tag{5}$$

The heat flux is determined by dividing the total heat input by the inner surface area [16], i.e.,

$$q^{"} = \frac{I \times V}{\pi D_i L} \tag{6}$$

The rate of heat transfer by convection ($q_c$) of the porous medium can be calculated by the Newton equation for cooling, namely,

$$q_c = h_{av} A_i (T_{iav} - T_b) \tag{7}$$

The average heat-transfer coefficient ($h_{av}$) can be calculated as follows

$$h_{av} = \frac{\mathring{m}Cp_f(T_{f,out} - T_{f,in})}{A_i(T_{iav} - T_b)} \tag{8}$$

where $T_b$ and $T_{iav}$ are the mean bulk temperature and inner tube temperature, respectively, measured as

$$T_b = \frac{1}{2}(T_{fi} + T_{fo}) \tag{9}$$

and

$$T_{iav} = \sum_{i=1}^{n} \frac{T_i}{n} \tag{10}$$

$A_o$ and $A_i$ are the inner surface area of the outer cylinder and the outer surface area of the inner cylinder, respectively; they are computed as follows

$$A_o = \pi D_o L \tag{11}$$

$$A_i = \pi D_i L \tag{12}$$

The average number of Nusselt ($N_{uav}$) can be calculated by heat-transfer coefficient ($h_{av}$), hydraulic diameter ($D_h$) and thermal conductivity coefficient ($k_{eff}$).

$$Nu_{av} = \frac{h_{av} D_h}{k_{eff}} \tag{13}$$

where

$$D_h = (D_o - D_i) \tag{14}$$

($k_e$) The total thermal conductivity of porous media is defined as a calculation method based on the thermal conductivity of fluid (water) and solid (balls) [17].

$$k_{eff} = \varepsilon k_f + (1-\varepsilon)k_s \quad (15)$$

where $k_f$ is the thermal conductivity of water, and $k_s$ is the thermal conductivity of glass spheres. (ε) The porosity of the porous medium is defined as the ratio of the total volume to the size of the test section.

$$\varepsilon = \frac{V_d - V_p}{V_d} \quad (16)$$

The area of the test section ($V_d$) is calculated as

$$V_d = \frac{\pi}{4}(D_o - D_i)L \quad (17)$$

The volume of glass spheres ($V_p$) is calculated as

$$V_p = \frac{4}{3}\pi r^3 n \quad (18)$$

Re can be calculated as

$$Re = \frac{4\dot{m}}{v_f} \quad (19)$$

The mass flow rate of water can be calculated by

$$\dot{m} = \rho_f Q \quad (20)$$

The flow rate Q is measured on the basis of mean fluid temperature using a flowmeter. The water density and water specific heat can be calculated. All fluid (water) properties in the annular tube are taken at average temperature ($T_m$) calculated by the arithmetic mean between the mean surface temperature of the internal and external cylinders along the annular tube as follows

$$T_m = \left(\frac{T_{iav} + T_{oav}}{2}\right) + 273.18 \quad (21)$$

The performance factor (σ) criterion is used as an improvement heat transfer for most passive techniques. It's computed as the ratio between the improvements of heat transfer to pressure drop [18,19] as

$$\sigma = \frac{\left(\frac{Nu_{por}}{Nu_{smo}}\right)}{\left(\frac{\Delta P_{por}}{\Delta P_{smo}}\right)^{1/3}} \quad (22)$$

Overall performance is better the higher the performance factor than one.

## 4. Result and Discussion

### *4.1 Verification of the Numerical Model*

Numerical results are compared with the experimental results of an annular tube filled with porous media. In Figure 6(a), the temperature of the fluid coming out of the annular tube is compared with the numerical and experimental results. The ratio of convergence between the numerical and experimental results is 0.25% for glass balls with a diameter of 11 mm. In Figure 6(b), a comparison of the average Nu for numerical and experimental values is made. Convergence between the numerical and experimental results is 6% for glass balls with a diameter of 16 mm. In Figure 6(c), the pressure drop is compared with the numerical and experimental values. The ratio of convergence between the experimental and numerical results is 18% for glass balls with a diameter of 25 mm. The reasons for the difference between the experimental and numerical results are the uncertainty in the measuring instruments and the assumptions imposed by the numerical simulations. The highest error ratio between the numerical and experimental results is 18%.

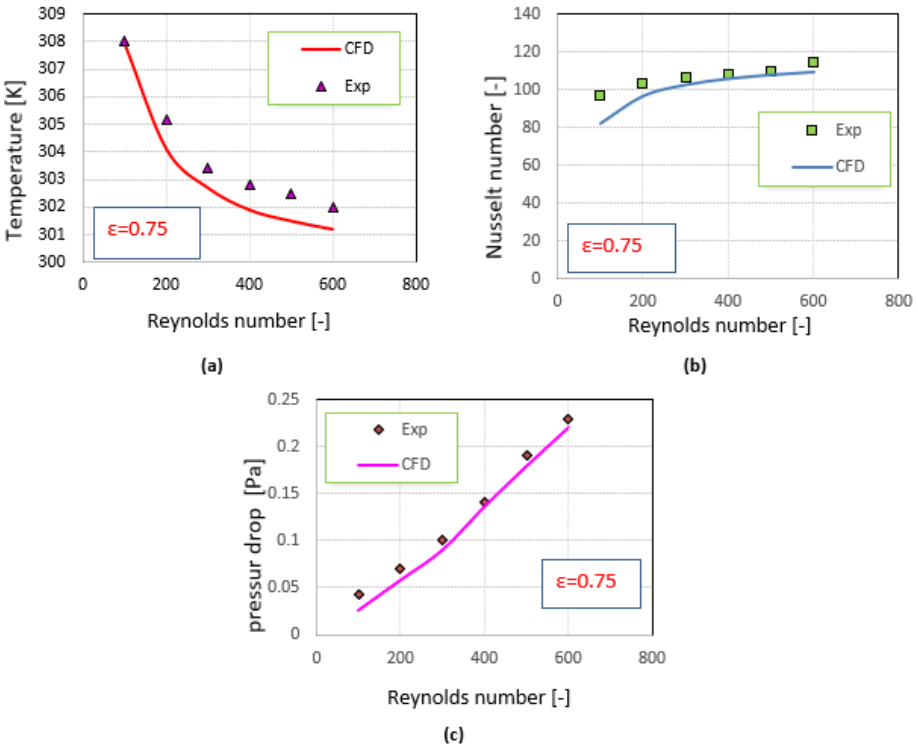


**Fig. 6.** Comparisons between the numerical and experimental results; (a) outlet water temperature with Re for d=11 mm, (b) Nu with Re for d=16 mm, (c) pressure drop with Re for d=25 mm

### *4.2 Temperature Distribution*

The temperature distribution along the annular tube filled with a porous medium between the surfaces of the inner and outer cylinders of the solid and liquid parts at Ti = 300 K at the entrance, a constant heat flux of q = 20 kW/m2 and the value of Re of 600 are considered. Figure 7 shows that the plane of (x, z) is taken along the fluid domain for the annular tube, and the axis is y = 0. For all cases, the temperature of the water at the entry is 300 K. The layer contacts the internal tube which represents the thermal flow that the temperature begins to rise gradually towards z-axis. Consequently, the water begins to gain heat when entering and reaches the central area, because

the transfer of heat at the middle is different from that at the entrance. The heat is reduced at the middle, and the water starts to gain heat from the constant thermal flux with the maximum heat exchange. The water is gaining heat whilst moving towards z-axis. The lowest heat value is at the input and the highest temperature value is at the output of z-axis. The highest heat transfer is at the beginning of z-axis, because the temperature is low. Whilst approaching z-axis, the temperature increases, whereas the heat transfer decreases. As for x-axis, the highest temperature is at the contact line of the internal tube. The temperature decreases whilst moving towards x-axis, because the effect of thermal flux is large at the contact area and less as x-axis is approached. The highest temperature is in the glass spheres at the diameter of 25 mm compared with those in the glass balls with diameters of 11 and 16 mm. This condition is due to the increase in the area of heat transfer between the water and the heat flux. Thus, the water reaches the highest temperature in the process of heat transfer from the heat flux. In all previous figures, the temperature is the lowest at the input, and the highest heat value is at the exit along z-axis. As for x-axis, the temperature is high at the contact area and gradually decreases towards x-axis.

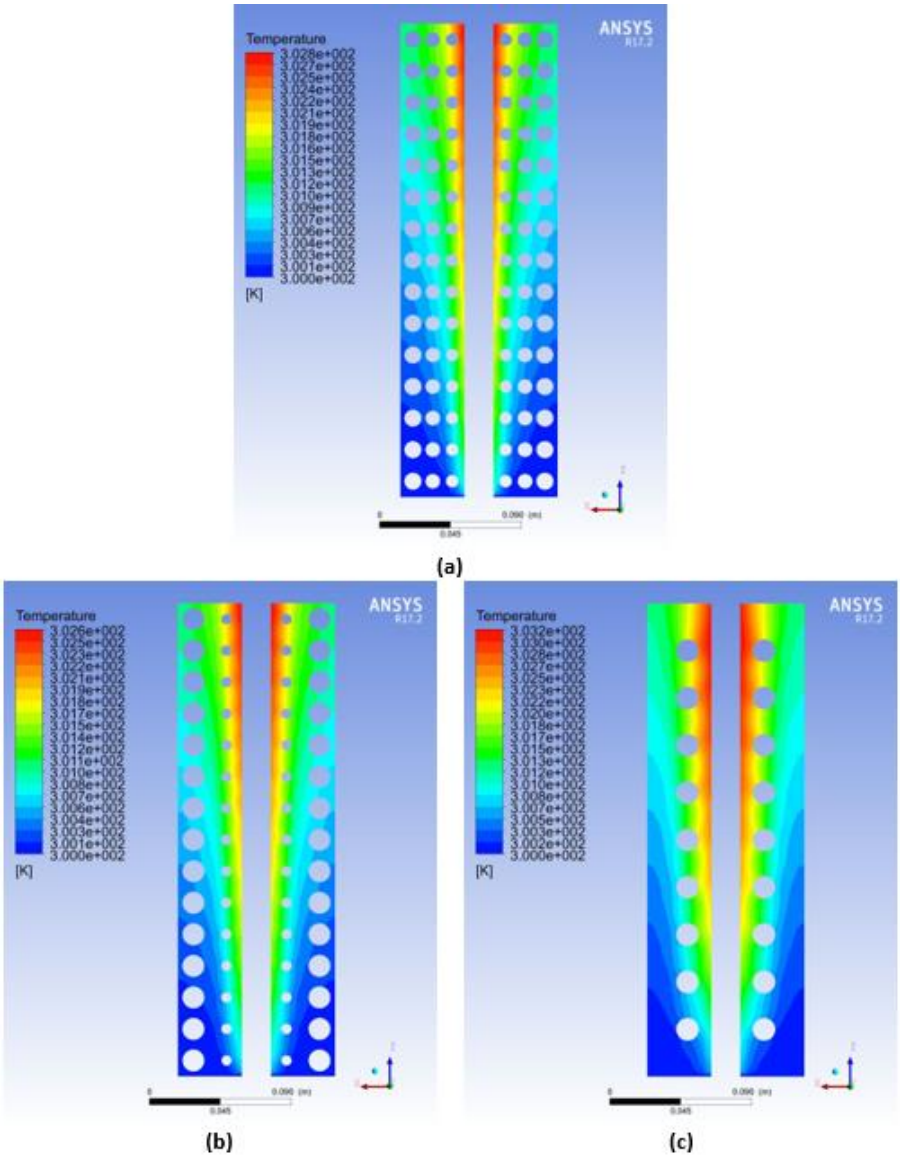


**Fig. 7.** Temperature distribution from plane along the fluid domain annular tube with different of diameters: (a) d=11 mm, (b) d=16 mm, (c) d=25 mm

### *4.3 Velocity Distribution*

The distribution of velocity along the annular tube filled with porous materials between the surfaces of the external and internal cylinders of the liquid and solid at the imposition of the speed of entry is 0.0042 m/s, and the discharge of a constant heat flux value is 20 kW/m2 at Re = 600. Figure 8 shows that the plane (x, z) is taken along the annular tube, and the axis is y = 0. For all cases, the speed begins to rise along z-axis and varies from one region to another. The speed is high from the area close to the surface of the internal cylinder and among the spaces of the balls. The value is low in the collision zone of the balls as a result of the collision of water velocity with the porous glass balls along z-axis. As for x-axis, the velocity is high at the contact area with the internal cylinder surface and starts to slow when colliding with the balls whilst moving towards x-axis. Finally, the water speed decreases when it hits the porous medium and increases at the space among the spheres along the annular tube.

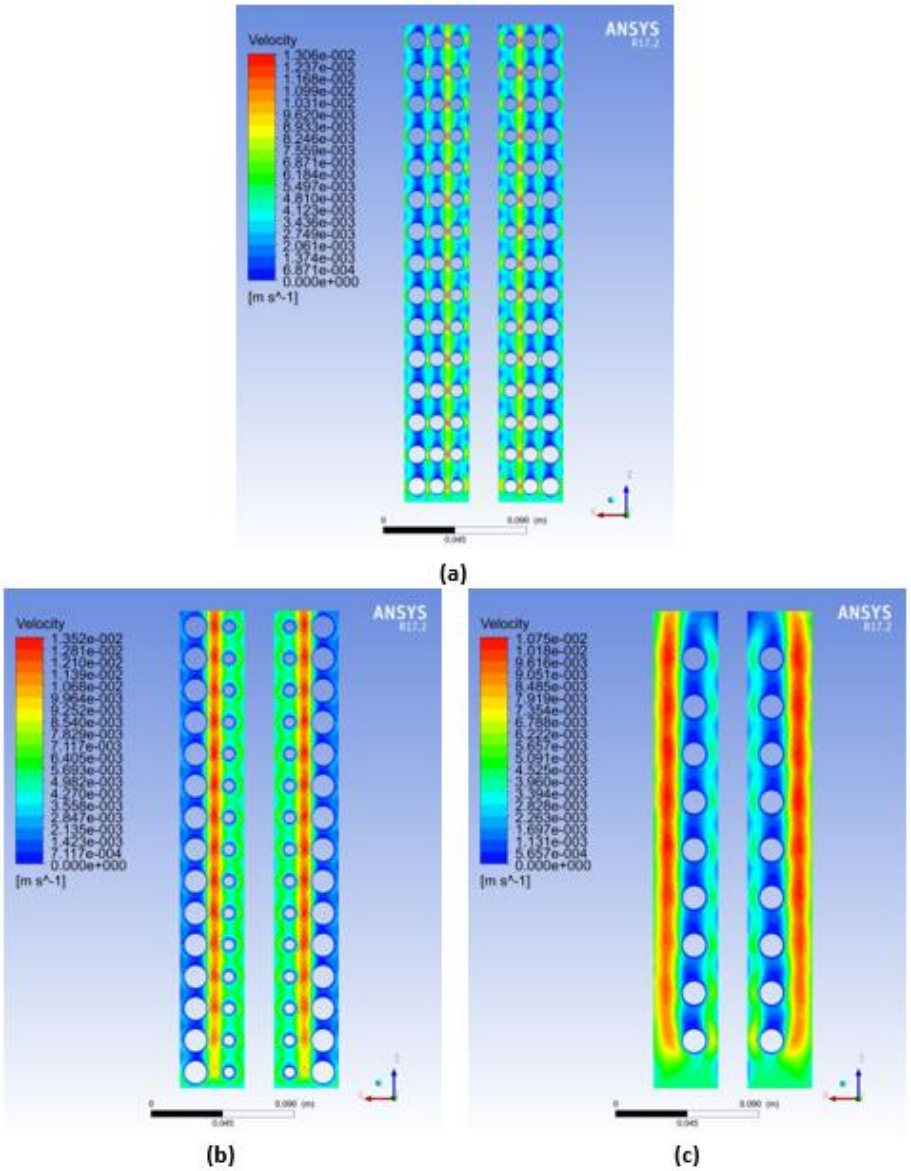


**Fig. 8.** Velocity distribution from plane along the fluid domain annular tube with different of diameter: (a) d=11mm, (b) d=16mm, (c) d=25mm

### *4.4 Effect of Porous Diameter*

Three different diameters (11, 16 and 25 mm) of glass balls are used to study their effect on the hydraulic and thermal performances of the concentric annular tube filled with a porous medium. The different diameters are the variable part, whereas porosity (ε = 0.75) is the constant value. Figure 9 to Figure 12 show the effect of Re on Nu, pressure drop, external fluid temperature and performance factor in the annular tube filled with porous materials. The value of the heat flux is confirmed at 150 kW/m2. Figure 9 shows the variation in Nu with Re for the annular tube filled with glass spheres with different diameters. Nu increases with increased Re for all cases. The value of Nu in the condition of the annular tube without the porous medium is small compared with that in the presence of porous materials. The increase in Nu can be attributed to the high conductivity of glass balls. Nu enhances with the presence of porous materials, which causes high heat transfer because of the high conductivity of the porous medium. The highest values of Nu are found at the glass balls with diameters of 11 and 16 mm. The increase in heat transfer for the diameter of 11 mm is 1420%, that for the diameter of 16 mm is 1474%, and that for the diameter of 25 mm is 1310%. Figure 10 shows the variation in pressure drop with Re in the annular tube filled with a porous medium and in the annular tube not filled with porous materials. The pressure drops increases within the annular tube with increased Re in the presence or absence of porous materials. A lower diameter of the glass spheres means a greater decrease in pressure drop with increased Re. The highest-pressure drop is at the glass balls with a diameter of 11 mm, compared with glass balls with diameters of 16 and 25 mm. The pressure drops increases by reducing the diameter and porosity of the balls. A lower diameter of the spheres means less space among the balls, thereby reducing the fluid flow and increasing the pressure drop. The increase in pressure drop for 11 mm diameter is 7303%, that for 16 mm diameter is 3450%, and that for 25 mm diameter is 1200%. Figure 11 shows the temperature variation of the outlet fluid in the annular tube filled with glass spheres with Re. The fluid temperature is inversely proportional with increasing in Reynolds number in all cases. The decrease in fluid temperature is due to the enhance in heat transfer in the annular tube as a result of the repeated re-mixing of the fluid inside the tube. The process of heat exchange with low water temperature is thus enhanced when increasing Re. Figure 12 shows the variation of the performance factor of the annular tube filled with porous materials. The performance factor begins to increase with increased Re. The performance factor also increases with decreased diameter of the balls from 25 mm to 11 mm. The best performance factor is achieved at the porous medium with a diameter of 25 mm. The performance factor begins to decrease with a reduction in the diameter of the porous materials. Convection heat transfer increases with increased diameter of the porous media owing to the high porosity and heat conductivity of the glass spheres, which increase the performance factor of the annular tube. The heat transfer behavior is different from the fluid flow behavior. The best heat-transfer diameter is 11 mm, and the best fluid diameter is 25 mm. Therefore, the best performance factor is at the porous medium with a diameter of 25 mm.

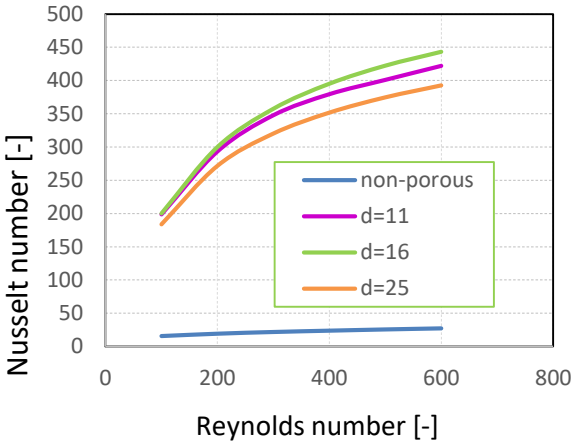


**Fig. 9.** Variations in Nu with Re for different diameters

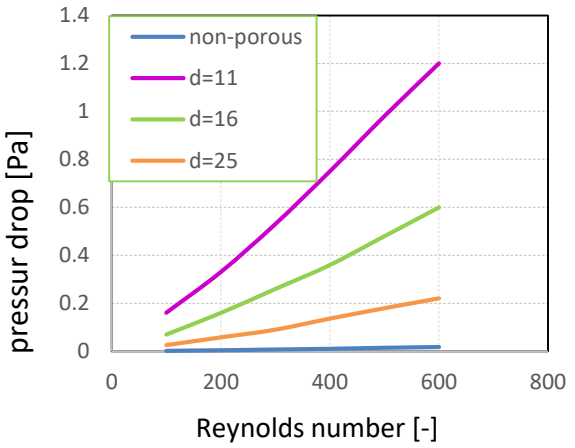


**Fig. 10.** Variations in pressure drop with Re for different diameters

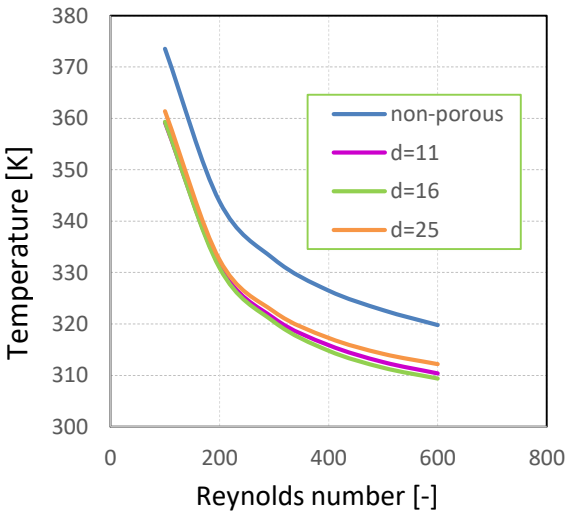


**Fig. 11.** Variations in the temperature of fluid outlet with Re for different diameters

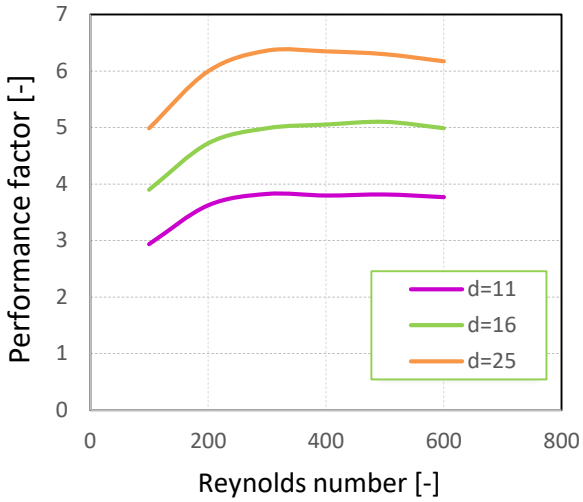


**Fig. 12.** Performance factor variations as a function of Re for different diameters

### *4.5 Effect of Porosity*

Three different values of porosity (0.65, 0.75 and 0.85) are used to study their effect on the performance of heat transfer in the annular tube filled with a porous medium. The diameter of the porous medium is stabilised at 25 mm, and the different porosity values are the variable part. Figure 13 to Figure 16 illustrate the Re effects on Nu, pressure drop, the temperature of the outside water, the performance factor in the annular tube filled with porous media and the porous medium with a diameter of 25 mm. Three different porosity values are used, with the heat flux at the value of 150 kW/m2. Figure 13 shows the variation in Nu with Re of the annular tube filled with a porous medium. Nu increases with increasing Re in the presence and absence of porous materials. The values of Nu are small in the annular tube without porous materials, whereas the values of Nu increase in the annular tube filled with porous media. Nu increases with the low porosity of the glass spheres. The highest value of Nu is found at the porosity of 0.65 because of the high conductivity of the glass balls inside the annular tube, which causes high heat transfer, compared with the annular tube without porous medium. The increase in heat transfer for the porosity of 0.65 is 1368%, that for the porosity of 0.75 is 1310%, and that for the porosity of 0.85 is 1227%. Figure 14 shows the pressure drop variation with Re of the annular tube filled with a porous medium. The pressure drops increases with increased Re in the presence and absence of the porous media in the annular tube. Pressure decreases with the use of glass balls with different porosities. The effect on pressure drop is evident as pressure decreases with a reduction in the porosity of the glass spheres. The highest-pressure drop is found at the porosity of 0.65. The pressure drop is low in the annular tube without porous medium. Pressure drop increases when the balls are added. Pressure drop is inversely proportional with the porosity. The increase in pressure drop for the porosity of 0.65 is 1431%, that for the porosity of 0.75 is 1209%, and that for the porosity of 0.85 is 765%. Figure 15 illustrates the variation in water outlet temperature from the annular tube filled with a porous medium with Re. The water temperature decreases with increased Re in the presence of porous medium in the annular tube. Low temperatures occur whilst Re increases in the absence of spheres in the annular tube. Three different values are used for the porosity of porous media. The effect of porosity on liquid temperature in the two cases is shown. Water temperature is reduced because of the high conductivity of the glass spheres that cause high heat transfer, thereby increasing heat exchange with low water temperature and Re in the annular tube. Figure 16 shows the variation in performance factor with Re in the annular

tube filled with a porous medium with a diameter of 25 mm. Three different values for the porosity of the glass spheres (0.65, 0.75 and 0.85) are used. The performance factor enhances as Re and the porosity of the porous medium increase. The best performance factor is achieved when the glass balls have porosity of 0.85. Convection heat transfer increases with increased porosity of the porous media, which is affected by the heat-transfer process. The performance factor of the annular tube filled with a porous medium is then increased.

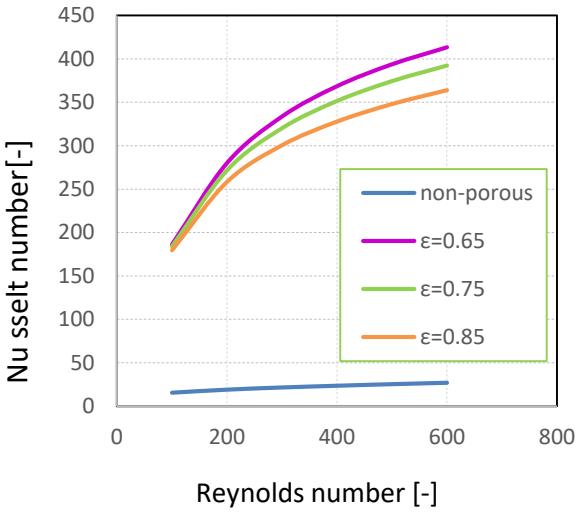


**Fig. 13.** Variations in Nu as a function of Re under different porosities

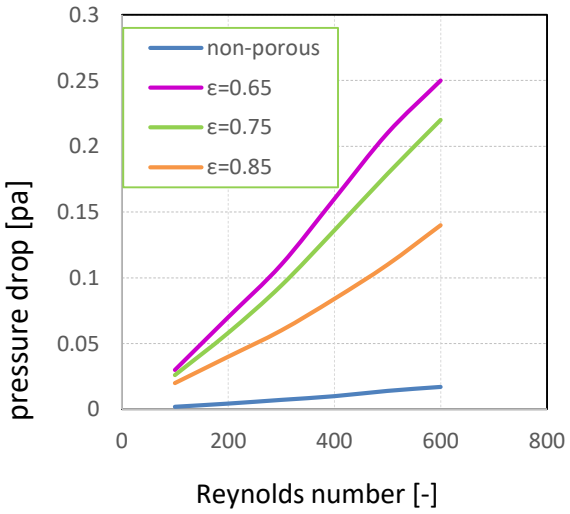


**Fig. 14.** Variations in pressure drop with Re under different porosities

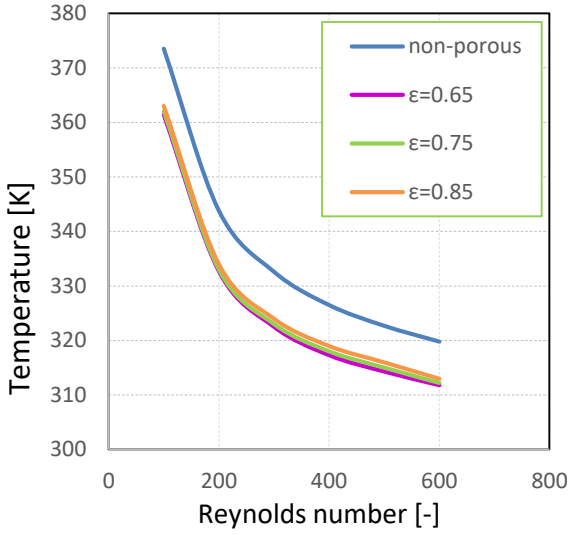


**Fig. 15.** Variations in the temperature of fluid outlet with Re under different porosities

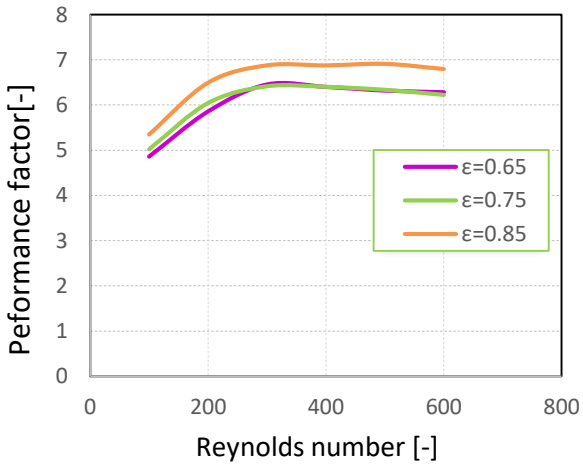


**Fig. 16.** Performance factor variations as a function of Re under different porosities

## 5. Conclusions

This work focused on the development numerical model and validated by fabrication of a test rig model to enhance the characteristics and performance of forced convection into vertical annuli with and without porous media. The numerical results were verified by comparing with experimental results, and good consistency was found in behaviour and values with a maximum deviation of 18% for pressure drop. The results of this research have different important conclusions that can be included

i. For all cases, the outlet water temperatures decrease with the Reynolds number increases and the highest temperature values at the smallest glass spheres diameter and highest porosity.
ii. For all cases, the Nusselt number is proportional with Reynolds number and the highest Nusselt number enhancement occurs at diameter of 25 mm about 4.5 times and the highest

Nusselt number enhancement occurs at porosity 0.65 and about 4.25 times. Compared than other glass balls diameters and porosities.

iii. The pressure drops increases with Reynolds number increase in all cases and the highest pressure drop at diameter 11 mm about 730 times and the highest pressure drop at porosity 0.65 about 143 times with those other cases.

iv. The performance factor of forced convection through vertical porous annulus is about 3 to 7 times higher than that annulus without porous media.

v. The optimum performance factor occurs at glass ball diameter of 25 mm and porosity of 0.85.

## References

[1] Bu-Xuan, Wang, and Du Jian-Hua. "Forced convective heat transfer in a vertical annulus filled with porous media." *International Journal of Heat and Mass Transfer* 36, no. 17 (1993): 4207-4213. https://doi.org/10.1016/0017-9310(93)90083-I

[2] Yang, C., F. Kuwahara, W. Liu, and A. Nakayama. "Thermal non-equilibrium forced convective flow in an annulus filled with a porous medium." *The Open Transport Phenomena Journal* 3, no. 1 (2011): 31-39. https://doi.org/10.2174/1877729501103010031

[3] Chikh, Salah, and Nadia Allouache. "Optimal performance of an annular heat exchanger with a porous insert for a turbulent flow." *Applied Thermal Engineering* 104 (2016): 222-230. https://doi.org/10.1016/j.applthermaleng.2016.05.069

[4] Cui, Y. J., B. L. Wang, K. F. Wang, and L. Zheng. "Power output evaluation of a porous annular thermoelectric generator for waste heat harvesting." *International Journal of Heat and Mass Transfer* 137 (2019): 979-989. https://doi.org/10.1016/j.ijheatmasstransfer.2019.03.157

[5] Shirvan, Kamel Milani, Rahmat Ellahi, Soroush Mirzakhanlari, and Mojtaba Mamourian. "Enhancement of heat transfer and heat exchanger effectiveness in a double pipe heat exchanger filled with porous media: numerical simulation and sensitivity analysis of turbulent fluid flow." *Applied Thermal Engineering* 109 (2016): 761-774. https://doi.org/10.1016/j.applthermaleng.2016.08.116

[6] Shirvan, Kamel Milani, Soroush Mirzakhanlari, Soteris A. Kalogirou, Hakan F. Öztop, and Mojtaba Mamourian. "Heat transfer and sensitivity analysis in a double pipe heat exchanger filled with porous medium." *International Journal of Thermal Sciences* 121 (2017): 124-137. https://doi.org/10.1016/j.ijthermalsci.2017.07.008

[7] Nimvari, Majid Eshagh, and Nima Fallah Jouybari. "Investigation of turbulence effects within porous layer on the thermal performance of a partially filled pipe." *International Journal of Thermal Sciences* 118 (2017): 374-385. https://doi.org/10.1016/j.ijthermalsci.2017.05.006

[8] Rong, Fumei, Wenhuan Zhang, Baochang Shi, and Zhaoli Guo. "Numerical study of heat transfer enhancement in a pipe filled with porous media by axisymmetric TLB model based on GPU." *International Journal of Heat and Mass Transfer* 70 (2014): 1040-1049. https://doi.org/10.1016/j.ijheatmasstransfer.2013.11.028

[9] Sheikhnejad, Yahya, Amir B. Ansari, Jorge Ferreira, and Nelson Martins. "Effects of parallel magnet bars and partially filled porous media on magneto-thermo-hydro-dynamic characteristics of pipe ferroconvection." *International Journal of Heat and Mass Transfer* 136 (2019): 1273-1281. https://doi.org/10.1016/j.ijheatmasstransfer.2019.03.085

[10] Boulechfar, Hichem, and Mahfoud Djezzar. "Thermosolutal natural convection in horizontal elliptical annulus containing a fluid-saturated porous medium: Effects of aiding buoyancy for low Rayleigh-Darcy number." In *Proceedings of the World Congress on Engineering*, vol. 2. 2014.

[11] Yang, Chen, Akira Nakayama, and Wei Liu. "Heat transfer performance assessment for forced convection in a tube partially filled with a porous medium." *International Journal of Thermal Sciences* 54 (2012): 98-108. https://doi.org/10.1016/j.ijthermalsci.2011.10.023

[12] Jha, Basant K., Deborah Daramola, and Abiodun O. Ajibade. "Mixed convection in a vertical annulus filled with porous material having time-periodic thermal boundary condition: steady-periodic regime." *Meccanica* 51, no. 8 (2016): 1685-1698. https://doi.org/10.1007/s11012-015-0328-4

[13] Roy, Nepal C., and Rama Subba Reddy Gorla. "Natural convection of a chemically reacting fluid in a concentric annulus filled with non-Darcy porous medium." *International Journal of Heat and Mass Transfer* 127 (2018): 513-525. https://doi.org/10.1016/j.ijheatmasstransfer.2018.08.061

[14] Tirandaz, Nima, Maziar Dehghan, and Mohammad Sadegh Valipour. "Heat and fluid flow through a helical annulus enhanced by a porous material: A perturbation study." *Applied Thermal Engineering* 112 (2017): 1566-1574. https://doi.org/10.1016/j.applthermaleng.2016.09.113

[15] Vatanparast, Mohammad Amniyeh, Siamak Hossainpour, Alireza Keyhani-Asl, and Sadra Forouzi. "Numerical investigation of total entropy generation in a rectangular channel with staggered semi-porous fins." *International Communications in Heat and Mass Transfer* 111 (2020): 104446. https://doi.org/10.1016/j.icheatmasstransfer.2019.104446

[16] Baragh, Shahram, Hossein Shokouhmand, Seyed Soheil Mousavi Ajarostaghi, and Mohammad Nikian. "An experimental investigation on forced convection heat transfer of single-phase flow in a channel with different arrangements of porous media." *International Journal of Thermal Sciences* 134 (2018): 370-379. https://doi.org/10.1016/j.ijthermalsci.2018.04.030

[17] Shahsavar, Amin, Abdullah A. A. A. Al-Rashed, Sajad Entezari, and Pouyan Talebizadeh Sardari. "Melting and solidification characteristics of a double-pipe latent heat storage system with sinusoidal wavy channels embedded in a porous medium." *Energy* 171 (2019): 751-769. https://doi.org/10.1016/j.energy.2019.01.045

[18] Hung, Tu-Chieh, Yu-Xian Huang, and Wei-Mon Yan. "Thermal performance analysis of porous-microchannel heat sinks with different configuration designs." *International Journal of Heat and Mass Transfer* 66 (2013): 235-243. https://doi.org/10.1016/j.ijheatmasstransfer.2013.07.019

[19] Pourfarzad, E., K. Ghadiri, A. Behrangzade, and Mehdi Ashjaee. "Experimental investigation of heat transfer and pressure drop of alumina-water nano-fluid in a porous miniature heat sink." *Experimental Heat Transfer* 31, no. 6 (2018): 495-512. https://doi.org/10.1080/08916152.2018.1451413